

Evaluation of snow depth and snow-cover over the Tibetan Plateau in global reanalyses using in-situ and satellite remote sensing observations

5 Yvan Orsolini¹, Martin Wegmann², Emanuel Dutra³, Boqi Liu⁵, Gianpaolo Balsamo⁴, Kun Yang^{6,7},
Patricia de Rosnay⁴, Congwen Zhu⁵, Wenli Wang^{6,7}, Retish Senan⁴, Gabriele Arduini⁴

1 NILU - Norwegian Institute for Air Research (Norway)

2 Alfred Wegener Institute, Helmholtz Centre for Polar and Marine Research (Germany), formerly at Institut des
10 Geosciences de l'Environnement, University of Grenoble, Grenoble, France

3 Instituto Dom Luiz (IDL), Faculdade de Ciências, Universidade de Lisboa, Portugal)

4 European Centre for Medium-Range Weather Forecasts (ECMWF) (United Kingdom)

5 Institute of Climate System, Chinese Academy of Meteorological Sciences, (China)

6 Department of Earth System Science, Tsinghua University (China)

15 7 Institute of Tibetan Plateau Research of Chinese Academy of Sciences (China)

Correspondence to: Yvan Orsolini (orsolini@nilu.no)

Abstract. The Tibetan Plateau (TP) region, often referred to as the Third Pole, is the world highest plateau and exerts a considerable influence on regional and global climate. The state of the snowpack over the TP is a major research focus due to its great impact on the headwaters of a dozen major Asian rivers. While many studies have attempted to validate
20 atmospheric re-analyses over the TP area in terms of temperature or precipitation, there have been –remarkably– no studies aimed at systematically comparing the snow depth or snow cover in global re-analyses with satellite and in-situ data. Yet, snow in re-analyses provides critical surface information for forecast systems from the medium to sub-seasonal time scales. Here, snow depth and snow cover from 4 recent global reanalysis products are inter-compared over the TP region, namely the European Centre for Medium-Range Weather Forecasts (ECMWF) ERA5 and ERA-Interim re-analyses, the Japanese
25 Re-Analyses (JRA-55) and the NASA Modern-Era Retrospective analysis for Research and Applications (MERRA-2). The re-analyses are evaluated against a set of 33 in-situ station observations, as well as against the Interactive Multi-sensor Snow and Ice Mapping System (or IMS) snow cover and a satellite microwave snow depth dataset. The high temporal correlation

coefficient (0.78) between the IMS snow cover and the in-situ observations provides confidence in the station data despite the relative paucity of in-situ measurement sites and the harsh operating conditions.

While several re-analyses show a systematic over-estimation of the snow depth or snow cover, the reanalyses that assimilate local in-situ observations or IMS snow-cover are better capable of representing the shallow, transient snowpack over the TP region. The later point is clearly demonstrated by examining the family of re-analyses from the ECMWF, of which only the older ERA-Interim assimilated IMS snow cover at high altitudes, while ERA5 did not consider IMS snow cover for high altitudes. We further tested the sensitivity of the ERA5 land model in off-line experiments, assessing the impact of blown snow sublimation, snow cover to snow depth conversion and, more importantly, excessive snowfall. These results suggest that excessive snowfall might be the primary factor for the large overestimation of snow depth and cover in ERA5 reanalysis. Pending a solution for this common model precipitation bias over the Himalayas and TP, future snow reanalyses that optimally combine the use of satellite snow cover and in-situ snow-depth observations in the assimilation and analysis cycles have the potential to improve medium-range to sub-seasonal forecasts for water resources applications.

1 Introduction

Often referred to as the Third Pole, the Tibetan Plateau (TP) region is the world highest plateau, with an average elevation of 4000 m above sea level. Due to its spatial extent, elevation and geographical position in the mid-latitudes, it exerts a considerable influence on regional and global climate. The formation and variability of the Asian summer monsoon in particular, is affected by the TP through thermal and mechanical effects (Wu et al., 2012, 2015; Xiao and Duan, 2016), with remote impacts both downstream (e.g., Zhang et al., 2004; Xue et al., 2018) and upstream (Lu et al., 2017). In autumn or winter, snow anomalies over the TP have been linked to wave trains extending downstream over East Asia and the Pacific (Liu et al., 2017; Li et al., 2018). Given its importance for climate and given that climate change strongly affects the region (Yang et al., 2014), the cryosphere over the TP is closely monitored in terms of glacier shrinking (Yao et al., 2012; Treichler et al., 2018), lake expansion (Zhang et al., 2017; Treichler et al., 2018) or change in the snowpack (Chen et al., 2017; Wang et al., 2017; Wang et al., 2018). The extent and variability of the snowpack over the TP has been a major focus of investigation because of the role of snow in the surface energy balance and in the hydrological cycle, as well as its potential impact on the large-scale circulation through radiative or thermodynamical feedbacks (Xiao and Duan, 2016; Lin et al., 2016; Henderson et al., 2018). In addition, water storage over the TP area affects the headwaters of a dozen major Asian rivers, affecting the livelihood of 22 % of the world population (Immerzeel et al., 2010). Several studies have aimed at quantifying the seasonal, interannual and decadal variability of the TP snowpack (e.g., Basang et al., 2017 and references therein). The seasonal snow cover over the TP is unique compared to other mid-latitude regions or to higher latitudes, because of its location in the 27° N - 40° N latitude belt, its high elevation and its distinct shallow, patchy and short-lived snowpack. In addition, the TP also receives a high amount of solar radiation, hence the short-wave snow albedo effect tends to be strong over that region. The TP is also a challenging region for snow-related research due to the complex terrain and the relative paucity of in-situ observation stations in this vast, sparsely populated expanse, especially in its western part.

There is, nevertheless, a substantial number of meteorological stations over the TP region, operated by the Chinese Meteorological Administration (CMA), which have been used in many climatological studies (e.g., for recent studies, Basang et al., 2017; Li et al., 2018). Since most of the stations are located in inhabited valleys, below 4000 m, in the southeast TP, the representativeness of these in-situ data for the TP as a whole is questionable.

5 Advances in satellite remote sensing have however provided invaluable information on the state of this high-elevation snowpack (Basang et al., 2017; 2018; Yang et al., 2015; Menegoz et al., 2013), often through blending data from multiple instruments to combine the high spatial resolution of optical data with the all-weather capability of microwave (MW) data. Since 2004, NOAA has provided an operational, daily, multi-sensor snow cover product (the Interactive Multisensor Snow and Ice Mapping System or IMS) at a high-resolution (4 km), by combining optical, infrared and MW satellite data and
10 surface observations (Helfrich et al., 2007). The accuracy of the IMS product compared to station data over the TP has been evaluated by Yang et al. (2015) and Li et al. (2018), who found the pixel matching accuracy (snow or no snow) to be over 90 %. Another widely used satellite optical product is the Moderate-resolution Imaging Spectroradiometer (MODIS) 8-day snow cover (Riggs and Hall, 2015; Basang et al., 2017). Joint analysis of MODIS and station data by Basang et al. (2017) indicated that, despite large day-to-day snow cover fluctuations and the non-synchronicity of these two datasets, there is a
15 high temporal correlation (0.77), if the station data is pre-processed in 8-day bins in a similar fashion as the MODIS data, i.e., if the station data is considered snow-covered in the 8-day period when snow covered for at least one day. Nevertheless, Basang et al. (2017) also showed that the spatial distribution of snow cover is uneven: the snow cover fraction is less than 21 % for 70 % of the TP area, and yet it can be up to 40 % in the eastern part of the TP. They also indicated a discrepancy in the seasonality of the maximum snow cover between station data and MODIS: the former had higher snow cover in the spring, when precipitation increases and falls as snow in the southeast TP. On the contrary, MODIS had a higher winter snow cover,
20 more representative of the mean conditions over the plateau. These latter discrepancies point out at large spatial differences in the characteristics of precipitation. Snow depth products are also available from satellite remotely sensing. Snow depth retrieval from MW observations is difficult in regions with complex topography, hampered by non-heterogeneity of snow grain size and of vegetation cover. Few MW snow depth products have been thoroughly evaluated over the TP, a region
25 characterised by a sparse and rapidly melting snowpack where, given the small snow grain size of fresh snow, the MW retrievals can lead to large errors (Dai et al., 2017). Nevertheless, a long-term MW snow depth product has been developed to account for the special conditions of the TP by Che et al. (2008) and Dai et al. (2017).

Atmospheric re-analyses comprehensively assimilate in-situ, balloon-borne, aircraft and satellite observations into a forecast model, and form an essential tool in meteorological and climate research (e.g., Bronnimann et al. 2018; Fujiwara et al.,
30 2017). Furthermore, re-analyses are sometimes used as initial conditions for seasonal hindcasts or reforecasts. A thorough up-to-date description and intercomparison of atmospheric re-analyses is found in Fujiwara et al. (2017). On the other hand, data assimilation in land surface models is performed separately from the atmospheric data assimilation due to the different nature of observations and methodologies involved (Hersbach et al., 2018). Early land re-analyses were performed as offline simulations without any actual assimilation of observations, but land data assimilation is rapidly evolving. For example, the

newest operational seasonal forecasting system 5 (known as SEAS5, Johnson et al. 2018) and the Integrated Forecast System (IFS) used for medium-range prediction at the European Centre for Medium-Range Weather Forecast (ECMWF), both rely on a land surface data assimilation system using a 2-dimensional optimal interpolation, which blends IMS snow cover and in-situ snow depth observations with the model background (de Rosnay et al., 2014, 2015). This evolution is partly motivated by the renewed interest in tapping into the potential of the land surface, and snow in particular, to improve the prediction skill at the subseasonal-to-seasonal time scale (Orsolini et al., 2013). Concerning the TP region more specifically, Lin et al. (2016) assimilated snow cover fraction from MODIS and/or water storage from GRACE in a land model and showed improvement in seasonal atmospheric temperature prediction resulting from the improved land conditions. The impact of realistic land initialization over the TP region on the Indian Summer Monsoon (ISM) has also been investigated (Senan et al., 2016; Halder et al., 2017; Rai et al., 2015). In particular, the impact of springtime initialisation on predicting the ISM onset was investigated by Senan et al. (2016) using the coupled ocean-atmosphere seasonal forecasting System 4 of the ECMWF. They found that, in years with anomalously high mean snow depth over the TP, as determined from the ECMWF land re-analyses, the ISM onset was delayed by about 8 days. Half of this delay was attributed to the initialization of snow over the TP region, highlighting the importance of land initialisation over that region for seasonal forecasting of the ISM onset.

While many studies have attempted to validate atmospheric re-analyses over the TP area in terms of temperature, precipitation or snowfall (Wang et al., 2012; Palazzi et al., 2013; Zou et al., 2014; Viste et al., 2015), there have been remarkably few studies aimed at evaluating and comparing the snow depth or snow cover in the re-analyses. Snow in long-term climate reanalyses over the plains of central and northern Russia have been evaluated against station data, showing surprisingly good performance (Wegmann et al., 2017). However, the terrain there is not as complex as over the TP. Previous studies of snow evaluation over the TP have focused purely on the remote sensing snow products (Basang et al., 2017; Yang et al., 2015; Dai et al., 2017). We argue that evaluation of snow re-analyses is of interest per se, since these re-analyses provide initial, critical surface information for the forecast systems, and link surface conditions with atmospheric dynamics.

The aim of this study is to compare snow cover and snow depth over the TP region among a set of modern atmospheric and land re-analyses, and to evaluate them against in-situ snow observations and selected satellite-based remote sensing products. A second goal is also to better characterise the snow biases in the re-analyses and to identify their origin. Sensitivity experiments are then carried out with a land surface model to assess the potential relevance of snow processes in driving the identified biases.

30

2 Data and methods

Maps of our study area with the orography at the resolution of the atmospheric re-analyses are shown in Figure 1. We make use of 3 re-analyses produced by ECMWF, namely the latest generation of atmospheric re-analyses (ERA5) (Hersbach et al., 2018), its older counterpart (ERA-Interim, hereafter ERA-I) (Dee et al., 2011), as well a land re-analysis obtained by running

the ECMWF land model (HTESSSEL) off-line, forced by the ERA5 meteorological forcing. Here, we refer to the latter as ERA5L-CTRL since it is not yet the officially released version of ERA5-Land expected to become available online in 2019 (<https://climate.copernicus.eu/climate-reanalysis>). In addition, we also make use of the Japanese Re-Analyses (JRA-55) (Kobayashi et al., 2015), and of the NASA Modern-Era Retrospective analysis for Research and Applications, Version 2 (MERRA2) (Gelaro et al., 2017). We did not carry out an exhaustive inter-comparison of all existing global re-analyses, but we chose the aforementioned analyses because they belong to the latest generation (ERA5, MERRA-2, JRA-55), or else because they incorporate either local snow observations over the TP region (JRA-55) or satellite snow cover observations that encompass the TP (ERA-I, JRA-55). Some general characteristics of these re-analyses are shown in Table 1, and more detailed information about the treatment and assimilation of snow variables is provided in the Appendix. Further information about the re-analyses systems can be found in Fujiwara et al. (2017) and Wright et al. (2018). For the evaluation of re-analyses, we use station data, the multi-sensor IMS snow cover product and satellite MW data, as detailed below.

2.1 Station Data

We obtained five years (2009 to 2013) of in-situ daily meteorological observations from 33 stations over the TP from CMA. The observations comprise minimum and maximum temperature, snow depth and total precipitation. The measuring time is 00:00 UTC (0800 Beijing time). The operational procedures dictate that, when more than 50 % of the ground surrounding the weather station is covered by snow, then the snow depth (SD) is measured. When converting in-situ snow depth to a snow cover fraction (SCF), a 100 % SCF is assumed when snow depth exceeds 1 cm, according to the in-situ observing rules of CMA (CMA, 2003). The in-situ observations also provide the snow cover days (SCD), i.e. the number of days when the snow covers more than 50 % of the ground in the sight from the station. The geographical locations of the stations are shown on Figure 1, along with their altitudes in comparison to the topography resolved by the four atmospheric re-analyses. Most of the stations are located in inhabited valleys, below 4000m, in the southeastern part and are not representative of the TP region as a whole. There is only one station in the western part of the TP, west of 85° E. In-situ observations have several sources of uncertainty. Here, we highlight two sources: (i) the stations might not be fully representative of their local surroundings due to the complex nature of the terrain, and (ii) the quality of the records could be affected by the harsh operating conditions. For example, strong winds limit the instrument ability to record the amounts of falling snow or solid precipitation, a phenomenon called undercatch.

2.2 Interactive Multisensor Snow and Ice Mapping System (IMS)

We use SCF from IMS, a multi-instrument, near-real time daily product covering the Northern Hemisphere with a pixel resolution of 4 km. IMS provides a binary (1/0) snow cover information: either 1 if more than 50 % of the 4-km pixel is covered by snow, or 0 (snow free) otherwise. Since, in this paper, we compare IMS data to re-analyses, we aggregate the 4-km product to a 0.25-degree grid, comparable to highest horizontal resolution among the re-analyses. This is done by

counting the number of pixels with a value of 1 in a grid-box, assuming they represent 100 % cover - this gives the "high estimate". If we assume that a value of 1 represents only 50 % of the 4 km pixel, we obtain the "low estimate", for which the maximum SCF possible is 50 %. These two estimates provide a range of values, reflecting the uncertainty inherent to aggregating the 4-km binary data, e.g., a value of 1 in a pixel means 50% to 100% snow coverage.

5 The choice of IMS snow cover is motivated by its use in the ECMWF analysis system. A key point is that it is used differently in ERA-I (Drusch et al., 2004) than in ERA5 (de Rosnay et al., 2014, 2015; Hersbach et al., 2018). First, the high-resolution 4 km product is used in ERA5, while the coarser resolution 24 km-product is used in ERA-I. More importantly, IMS data is not used above 1500 m in ERA5, i.e., in high altitude regions such as the TP, while it was still in use in ERA-I. When comparing the snow cover in IMS with the one in ERA-I or ERA5, one has to recall that these are not
10 independent datasets. Nevertheless, the different usage of IMS data between ERA5 and ERA-I allows to highlight the importance of snow cover analysis and assimilation over the TP. In that region, in-situ data available for the numerical weather prediction community for real time applications is still scarce.

2.3 Microwave satellite data

15 A long-term (1978-2010) MW daily snow depth product has been developed to account for the special conditions of the TP by Che et al. (2008) and Dai et al. (2017) at the Cold and Arid Regions Environmental and Engineering Research Institute (CAREERI) of the Chinese Academy of Sciences. We used the two years (2009 and 2010) that overlap with our comparison period (2009-2013), the latter dictated by our station data record. Over these two years, the MW product is based on measurements from the NASA Advanced Microwave Scanning Radiometer for Earth Observing System (AMSR-E). The
20 gridded dataset has a horizontal resolution of 0.25 degree.

3 Results

3.1. Snow depth

Figure 2 presents a comparison of daily SD over the 5-year period (2009-2013) between the observations, comprising both in-situ station and MW data, and the 4 re-analyses collocated at the station coordinates. The comparison is an average over
25 the 33 stations. The in-situ observations, even in the mean over all available stations, reveal a very thin and rapidly fluctuating snowpack, with episodes of fast build-up and decay, followed by periods void of snow, even in mid-winter. This concurs with previous studies showing that large parts of the TP can remain snow-free even in winter (Basang et al., 2017; Li et al., 2018). A quantitative estimate of the discrepancy between in-situ daily observations and the other datasets as a root-mean-square error (RMSE) is presented in Fig. 4 (left panel). The RMSE is calculated for the two years 2009 and 2010 when
30 satellite MW data is available. We also calculated the temporal correlation matrix between the different SD datasets (Table 2), using daily data year-round over the 5-year period, except for the satellite MW data where only the two years 2009 and 2010 are used. It is clearly apparent that, with the exception of MERRA-2, the re-analyses show a regular seasonal cycle, with a snowpack that grows nearly steadily during the cold season and culminates in February or March. This is unlike the

in-situ observations, which show rapidly fluctuating snow increases with little snow accumulation throughout winter. In comparison with in-situ observations, MERRA-2 has the best performance among re-analyses for both the RMSE and the temporal correlation, closely followed by JRA-55. The ERA5 re-analysis over-estimates the seasonal maximum SD by a factor of 10. Among the ECMWF family of re-analyses, the older ERA-I is performing best in terms of RMSE. Nevertheless, the temporal correlation is similar to the one obtained with ERA5, indicating that the newer, higher resolution ERA5 similarly captures the snow variability despite its large positive bias. The MW satellite data is also overestimating SD, as noted by Yang et al. (2015) or Dai et al. (2017). Like the re-analyses, it shows a progressive snow accumulation throughout the cold season. It also poorly captures short-term SD variability (Fig. 2) and its temporal correlation with the in-situ data is 0.32, poorer than for the re-analyses, even though calculated over only two years. The RMSE error is nevertheless comparable to ERA-I, and the MW data is able to estimate SDs smaller than 5 cm.

It is not surprising that JRA-55 performs well, since it assimilates SDs from a dozen CMA stations over the TP area and snow cover from satellite MW data (see Appendix). Note that the assimilated MW data is not from the same instrument as the one used in the CAREERI MW data. A key factor in the relatively good performance of ERA-I is the fact that it assimilates SCF from IMS in high-altitude regions, hence also over the TP. On the contrary, as mentioned earlier, assimilation of IMS SCF above 1500m was discontinued in the production of ERA5. Among the differences in the snow treatment between ERA-I and ERA5, the tendency to reduce or remove the snowpack imposed by the IMS observational constraint during assimilation appears the most likely key factor in bringing ERA-I SDs significantly closer to the in-situ observations.

3.2. Snow cover and snow maps

Figure 3 presents a comparison of daily SCF over the 5-year period (2009-2013) between the in-situ station observations and the IMS satellite data and the 5 re-analyses, collocated at the station coordinates. Again, an average over the 33 stations is presented. The IMS data is represented by the range between the low and high estimates (see Section 2). The correlation matrix and the RMSE for SCF are provided in Table 2 and in Fig. 4 (right panel) respectively, calculated over the 5-year period. There is good agreement between in-situ observations and the IMS low estimate: the station-mean year-round correlation (Table 2) over the 5 years (2009-2013) is 0.78. In Li et al. (2018), the correlations between SCF at 55 CMA stations and IMS SCF during the 10 winters between 2000 and 2010 ranged from 0.39 to 0.79, with a 10-winter average of 0.56. The consistency of the temporal correlation with Li et al. (2018) indicates that the satellite snow cover data readily captures the rapidly fluctuating snowy events. It also provides some confidence in the station data despite the harsh operating conditions for in-situ measurements, and the spatial degradation applied to IMS (from 4 km to 0.25 degree).

It is clearly apparent that ERA5 again considerably overestimates SCF. JRA-55 is much worse than MERRA-2 for SCF, while their performance for SD was similar. As described in the Appendix, the a-posteriori conversion from SD to SCF varies among re-analyses. For JRA-55, a thin 2 cm layer is equivalent to 100 % SCF, hence JRA SCF is persistently high; on the contrary, in MERRA-2, SCF values are small due to the large SD required to have full snow cover (see Appendix for details). While the in-situ station data (e.g., Fig. 3) also displays thin layers of a few cm, they are very transient. Further

validation is provided in terms of the annual-mean SCDs. Table 3 compares SCDs among the datasets, both for the 5-year average and for individual years, based on monthly-mean SCD values. The values of SCDs compare well between in-situ observation and IMS. On the other hand, ERA5 and JRA-55 re-analyses largely overestimate SCDs (ERA5 by nearly three times), while ERA-I is closer to the observed values. The temporal correlation coefficients for monthly SCDs tend to be higher than that for the daily SCF or SD. Note the values of SCDs in MERRA-2 are small due to the SCF being below the 0.5 threshold used in the SCD definition (see Fig. 3).

Moving to the geographical distribution over the TP region, Fig. 5 shows maps of the 5-year mean SD in January for each of the 4 re-analyses, with the in-situ data embedded in each map. January is chosen to illustrate a mid-winter month when snowfall is relatively common and differences between re-analyses are large. In the southeast TP, where the stations are located, MERRA-2, JRA-55 and ERA-I have SDs comparable to in-situ observations, as was shown in Fig. 2. In the western station-void part, there are also large differences in the snow depth (up to factor 5) among the re-analyses, especially along the arc of the Himalayas and other high mountain ranges. Figure 6 is similar to Fig. 5 but represents January anomalies from the satellite MW data for the combined years 2009 and 2010. In the southeastern part, SDs in MERRA-2, ERA-I and JRA-55 are smaller than the MW data, consistent with Fig. 2. Figure 6 also reveals that ERA5 and JRA-55 have an excessive SD over the high mountains of the Western Himalayas compared to satellite MW data, unlike ERA-I with its high-altitude snow cover assimilation. Figure 7 shows maps of the 5-year mean SCF in January for each of the re-analyses, for the two (low and high) estimates from IMS, again with the in-situ SCF embedded in the maps. While there is a good agreement between the in-situ data and the IMS low estimate, as shown earlier at station locations, the overestimation by ERA5 extends over the eastern and western parts of the TP. Nevertheless, some parts of Central Tibet and the Taklamakan desert to the north are snow-free in January in both IMS and most re-analyses. ERA-I agrees much better with the IMS data, while JRA-55 SCF is too high, due to the SD vs. SCF conversion as explained above. On the contrary, the MERRA-2 SCF is exceedingly low and featureless.

4 Discussion

4.1. Snow cover to snow depth conversion

A first important issue to mention is that the conversion of SD to SCF differs significantly among re-analyses. SCF is perhaps the most important snow-related climate driver for the surface budget, since the short-wave snow albedo feedback is strong on the TP, especially in the spring. The snowpack is also quite thin, so that thermodynamical feedbacks linked to snow thickness are less important. A 100 % SCF might correspond to snow depths ranging from 26 cm to 2 cm, depending on the re-analysis considered. There may also be some dependence on snow density as in the cases of ERA-I and MERRA-2. Hence, while JRA-55 has excellent performance among re-analyses for SD, the snow cover is exaggerated due to the conversion to 100 % SCF obtained with a small SD threshold value of 2 cm. While MERRA-2 SCF compares best with station data among the among re-analyses (see Fig. 4, right), being close to the low IMS estimate, it is exceedingly low over

the TP overall (Fig. 7), given the comparatively high value (26 kg m^{-2}) used for snow mass to get a fully covered snow area (Reichle et al. 2017a).

4.2. Sensitivity in off-line ERA5-land simulations

We carried out simple sensitivity off-line experiments with the ERA5 land model to shed some light on potential explanations for the large biases in the ERA5 reanalysis, which might be partly due to a missing snow removal process or to excessive snowy precipitation. Gordon et al. (2006) reported that blowing snow events are common in the Canadian Prairies and in the Arctic. As snow is carried out in suspension, it may sublimate. In a model study, Pomeroy and Li (2000) predicted that two-thirds of the snow transported from the surface to the atmosphere sublimates in the Prairie regions, and one-half in the Arctic regions. Brun et al. (2013) used Gordon's parameterization and argued that this was an important process in simulating snow dynamics in Northern Eurasia. Processes like the blowing of snow and the sublimation of the blown snow might be important processes in the windy and dry conditions of the TP. To test the hypothesis that sublimation of blowing snow is an important missing process, a simple parametrisation of blown snow sublimation has been introduced, as described in the Appendix. It has been tested for two wind thresholds for blowing snow initiation. Furthermore, the impacts of changing the threshold in the snow depth to snow cover conversion and of reducing snowfall were tested separately. Other processes such as the impacts of blown snow on surface roughness or of snow drifts were not tested. In addition to the ERA5L-CTRL run described in Sect. 2, we hence performed an additional set of 5 land-only experiments testing (i) the effect of snow sublimation due to blowing snow in BLW and in BLW_L with a lower threshold for blowing snow initiation, (ii) the 100 % SCF threshold, changed from 10 cm to 5 cm in SCF05, and to 20 cm in SCF20, and (iii) the excessive snowfall by reducing snowfall by 50 % in SNF50. These 5 experiments with ERA5-land, as summarized in Table 4, were carried for the period 1/1/2019 to 31/12/2014, and over the domain 60.125° E to 109.875° E and 25.125° N to 44.875° N , with a regular latitude/longitude resolution of 0.25° . The simulations were driven by the ERA5 meteorological fields interpolated to this regular grid.

The evaluation of the different budget terms over the 33-station mean snow depth and cover (Table 5) as well as the root mean square errors and the temporal correlation with observations (Table 6). These results indicate that (i) the offline simulation (CTRL) with the same configuration as ERA5 represents closely the errors found in ERA5 as expected, (ii) the effects of snow sublimation due to blowing snow and of the SCF threshold change are negligible, and (iii) artificially reducing snowfall by 50% reduces the systematic biases significantly, and increases the temporal correlation of snow depth as well. The temporal variability of snow cover is captured reasonably well by ERA5 and the other experiments, suggesting that the main dynamic features of snow accumulation and depletion are well represented.

4.3 Excessive precipitation issue

These results suggest that excessive snowfall might be a key responsible for the large overestimation of snow depth and cover in ERA5 reanalysis. Excessive snowfall over this region is in fact a common bias among climate and forecast models (Su et al., 2013). In fact, the largest relative climate model bias for precipitation over land, globally, is on the TP (Flato et al., 2013). In order to provide further evidence for the precipitation bias, we present in Fig. 8 the 5-year mean seasonal cycles of minimum temperature, maximum temperature, total precipitation rate (i.e. liquid and snowy precipitation), snow cover and snow depth, based on monthly means and averaged over all the 33 stations. Figure 8 reveals that all re-analyses have a cold temperature bias compared to in-situ observations, especially in maximum temperature, which is largely consistent with their respective thick snowpack bias. For example, ERA-I is warmer and closer to the in-situ observations than ERA5, likely due the latter having a higher snow depth. The good performance of ERA-I (and also of the first-generation MERRA) against in-situ station temperature data had been noted by Wang and Zeng (2012). All re-analyses have a precipitation excess (Fig. 8c), except MERRA-2 which uses observed precipitation data, including over the TP region. Incidentally, this may explain the excellent performance of MERRA-2 in terms of mean snow depth over the stations (see Fig. 4, left). Palazzi et al. (2013) also reported the precipitation excess in ERA-I, for example. In fact, ERA-I displays a precipitation excess greater than the more recent ERA5, despite having smaller SDs. The improvement in precipitation in ERA5 is likely due to its higher horizontal resolution, allowing better representation of synoptic events. Note that the precipitation seasonal cycle is largely dominated by summer monsoonal precipitation in the southeast TP. While our focus here is on the cold season, when precipitation is much smaller but likely falling as snow, there is still a positive bias in the re-analyses then, indicating excessive snowfall. It must be kept in mind though, that in-situ observations of snowfall are associated with a large uncertainty due to undercatch and other technical challenges.

Hence, a remaining question that must be addressed in future studies is the origin of the seasonal moisture transport to the TP region leading to the excess precipitation in models. While the results of the off-line sensitivity tests do not support a role for sublimation due to blowing snow, it could be that the local turbulent surface winds are much higher than in the re-analyses. Hence the importance of the blown snow sublimation cannot be fully discounted. We further note that there is a strong regional seasonality in the precipitation pattern over the TP. The wet season precipitation (May-September) accounts for more than 70 % of the total annual precipitation over the south and southeast TP (where stations are located), a region that falls under the influence of the Asian summer monsoon (Maussion et al., 2014). Over the western and northwest parts of the TP on the other hand, the wet season precipitation is less than 300 mm. This region is influenced by strong winter and spring westerlies and transient migratory synoptic eddies embedded in them, the so-called *westerly disturbances*, which provide a significant portion of the annual mean precipitation, especially over the Western Himalayas (Tiwari et al., 2017). An effective barrier effect, inhibiting large-scale moisture transport over the region, is not captured by any of the models underpinning the re-analyses used here. The impact of having higher model horizontal resolution to resolve the complex topography has to be considered. Lin et al. (2018) carried out simulations for the summer monsoon season with the weather research forecasting model (WRF) at resolutions of 30, 10 and 2 km, and found that the finest resolution (2 km) diminished

the water vapour transport to the TP, and the precipitation bias. They also noticed a large improvement when model resolution changed from 30 to 10 km. The insufficient subscale orography variance and orographic drag seems to be a key factor (Zhou et al., 2019). Based on these results, it appears that the highest resolution in atmospheric re-analyses examined here (near 32 km in ERA5) remains insufficient, as demonstrated by the precipitation excess compared to station data in Fig.

5 8c.

Finally, we note that the particular relevance of the western TP snowpack for subseasonal-to-seasonal prediction, due to the limited snowpack persistence over the eastern and central TP, as was already emphasized by Xiao and Duan (2016). Yet, with only one station in our inter-comparison, the western TP snowpack remains the less constrained by in-situ data, and further studies on this issue are warranted.

10 **5 Summary**

We have shown that several recent, state-of-the-art re-analyses produce an over-extensive snowpack in autumn, winter and spring over parts of the TP. This is at odds with observational studies revealing that snowfall events are very transient, that the snow cover vanishes rapidly on time scales of days, and that large parts of the TP can remain snow-free in winter (e.g., Basang et al., 2017; Li et al., 2018). The reanalyses that assimilate local in-situ observations or satellite snow-cover or
15 precipitation are better capable of representing the shallow, transient snowpack over the TP region. MERRA-2 and JRA-55 have the best performance among re-analyses for snow depth. Considering the family of re-analyses from the ECMWF, we surmise that the underperformance of ERA5 in terms of SD compared to its older counterpart ERA-I, is due to the lack of IMS data assimilation at high altitudes, including over the TP. This issue will be subject of a follow-up publication, using dedicated assimilation experiments. Pending a solution for the common model precipitation bias over the Himalayas and TP,
20 which may require much higher horizontal resolutions than currently used in global re-analyses, improved snow initialisation through better use of observations in the analyses may improve the medium-range to sub-seasonal forecasts.

Acknowledgment. We acknowledge the support of the International Space Science Institute in Beijing, through the working team “Snow reanalyses over the Himalaya-Tibetan Plateau region and the monsoons” over the years 2016-2018 (Team
25 leaders: Yvan Orsolini and Gianpaolo Balsamo). Emanuel Dutra was supported by the Portuguese Science Foundation (FCT) under project IF/00817/2015. Joaquín Muñoz Sabater is acknowledged for valuable comments on ERA5L testing. The lead author also acknowledges partial support from the Working Group on Subseasonal to Interdecadal Prediction (WGSIP) (<https://www.wcrp-climate.org/modelling-wgsip>) of the World Climate Research Programme (WCRP). We are also grateful to Shinya Kobayashi, Yayoi Harada, Rolf Reichle and Sujay Kumar for help with the re-analyses.

30

Author contribution. All co-authors participated to the analysis through the aforementioned working team. M. Wegmann and E. Dutra drafted the figures. B. Liu and C. Zhu analysed and provided the station data.

Data availability. All re-analyses data are publically available: MERRA-2 from NASA Goddard Earth Sciences Data and Information Services Center, ERA5/ERA-I/ERA-land from the European Centre for Medium-Range Weather Forecasts (ECMWF), and JRA-55 from the Japanese Meteorological Agency. The station data has been made available through the Chinese Meteorological Administration (CMA). IMS snow cover is publically available from NOAA, and the long-term
5 MW satellite data is available from CAREERI.

References

- Basang, D. K. : Snow Cover Distribution and Variation in Tibet, PhD thesis, University of Bergen. ISBN: 978-82-308-3713-9, 2018.
- Basang D., Barthel K., Olseth J. A.: Satellite and Ground Observations of Snow Cover in Tibet during 2001–2015, *Remote
10 Sensing*, 9(11):1201, 2017.
- Brun E. et al.: Simulation of Northern Eurasian Local Snow Depth, Mass, and Density Using a Detailed Snowpack Model and Meteorological Reanalyses, *J. Hydrom.*, 14, 203-219, 2013.
- Brönnimann S., R. Allan, C. Atkinson, R. Buizza, O. Bulygina, P. Dahlgren, D. Dee, R. Dunn, P. Gomes, V.O. John, S.
15 Jourdain, L. Haimberger, H. Hersbach, J. Kennedy, P. Poli, J. Pulliainen, N. Rayner, R. Saunders, J. Schulz, A. Sterin, A. Stickler, H. Titchner, M.A. Valente, C. Ventura, and C. Wilkinson : Observations for Reanalyses, *Bull. Amer. Meteor. Soc.*, **99**, 1851–1866, <https://doi.org/10.1175/BAMS-D-17-0229.1>, 2018.
- Che T., Li X., Jin R., Armstrong R. and Zhang, T.: Snow depth derived from passive microwave remote-sensing data in China, *Annals of Glaciology*, 49, 145-153, 2008.
- 20 Chen X., Long D., Hong Y., Liang S. and Hou A.: Observed radiative cooling over the Tibetan Plateau for the past three decades driven by snow cover-induced surface albedo anomaly, *J. Geophys. Res. Atmos.*, 122, 6170–6185, 2017.
- China Meteorological Administration: Ground Meteorological Observation Specifications (in Chinese). Beijing: China Meteorological Press, 151-153, 2003.
- Cressman G. P.: An operational objective analysis system, *Mon. Wea. Rev.*, 87.10: 367-374, 1959.
- 25 Dai L., Che T., Ding Y. and Hao X.: Evaluation of snow cover and snow depth on the Qinghai-Tibetan Plateau derived from passive microwave remote sensing, *The Cryosphere*, 11, 1933-1948, 2017.
- Dee D. P. et al.: The ERA-Interim reanalysis: configuration and performance of the data assimilation system, *Q. J. Roy. Meteor. Soc.*, 137, 553–597, 2011.
- de Rosnay P., Balsamo G., Albergel C., Muñoz-Sabater J. and Isaksen L.: Initialisation of land surface variables for
30 Numerical Weather Prediction, *Surveys in Geophysics*, 35(3), 607-621, doi: 10.1007/s10712-012-9207-x, 2014.
- de Rosnay P., Isaksen L., and Dahoui M.: Snow data assimilation at ECMWF, *ECMWF Newsletter*, no 143, pp 26-31, Spring 2015 (<https://www.ecmwf.int/sites/default/files/elibrary/2015/14587-newsletter-no143-spring-2015.pdf>), 2015.

- Drusch M., Vasiljevic D., and Viterbo P., : ECMWF's Global Snow Analysis: Assessment and Revision Based on Satellite Observations, *J. Appl. Meteor.*, 43, 1282–1294, 2004.
- Dutra E., Balsamo G., Viterbo P., Miranda P.M.A., Beljaars A., Schar C. and Elder K.: An improved snow scheme for the ECMWF land surface model: description and offline validation, *J. Hydrometeorol.*, 11:899–916, 2010.
- 5 Flato G., et al.: Evaluation of climate models. *Climate Change 2013 – The Physical Science Basis: Working Group I Contribution to the Fifth Assessment Report of the Intergovernmental Panel on Climate Change*, Cambridge University Press, pp.741-866. [10.1017/CBO9781107415324.020](https://doi.org/10.1017/CBO9781107415324.020) , 2013.
- Fujiwara M. et al.: Introduction to the SPARC Reanalysis Intercomparison Project (S-RIP) and overview of the reanalysis systems, *Atmos. Chem. Phys.*, 17, 1417–1452, 2017.
- 10 Gelaro R. et al.: The Modern-Era Retrospective Analysis for Research and Applications, Version 2 (MERRA-2), *J. Climate*, 30, 5419–5454, 2017.
- Gordon M., Simon K. and Taylor P.A.: On snow depth predictions with the Canadian land surface scheme including a parametrization of blowing snow sublimation, *Atmosphere-Ocean*, 44:3, 239-255, DOI: 10.3137/ao.440303, 2006.
- Halder S. and Dirmeyer P. A.: Relation of Eurasian Snow Cover and Indian Summer Monsoon Rainfall: Importance of the Delayed Hydrological Effect, *J. Climate*, 30, 1273-1289, 2018.
- 15 Helfrich S. R., McNamara D., Ramsay B. H., Baldwin T. and Kasheta T.: Enhancements to, and forthcoming developments in the Interactive Multisensor Snow and Ice Mapping System (IMS), *Hydrol. Process.*, 21: 1576-1586, 2007.
- 20 Henderson G. et al.: Snow–atmosphere coupling in the Northern Hemisphere, *Nature Climate Change*, 8, 954–963, 2018.
- Hersbach H. et al.: Operational global reanalysis: progress, future directions and synergies with NWP", *ECMWF ERA report series*, N27, December 2018 (<https://www.ecmwf.int/en/elibrary/18765-operational-global-reanalysis-progress-future-directions-and-synergies-nwp>), 2018.
- 25 Immerzeel W.W. et al.: Large-scale monitoring of snow cover and runoff simulation in Himalayan river basins using remote sensing, *Remote Sensing of Environment*, 113, 40–49, 2009.
- Johnson S.J., Stockdale T.N., Ferranti L., Balmaseda M.A., Molteni F., Magnusson L., Tietsche S., Decremmer D., Weisheimer A., Balsamo G., Keeley S., Mogensen K., Zuo H. and Monge-Sanz B.: SEAS5: The new ECMWF seasonal forecast system, *Geosci. Model Dev. Discuss.*, <https://doi.org/10.5194/gmd-2018-228>, in review, 2018.
- 30 Kobayashi S. et al.: The JRA-55 Reanalysis: General specifications and basic characteristics, *J. Meteorol. Soc. Jpn.*, 93, 5–48, doi: 10.2151/jmsj.2015-001, 2015.
- Li L. and Pomeroy J.W.: Probability of occurrence of blowing snow, *J. Geophys. Res.*, 102(D18), 21955–21964, doi:10.1029/97JD01522, 1997.
- 35 Li W., Guo W., Qiu B., Xue Y., Hsu P.-C. and Wei J.: Influence of Tibetan Plateau snow cover on East Asian atmospheric circulation at medium-range time scales, *Nature Comm*, 9:4243, DOI: 10.1038/s41467-018-06762-5, 2018.
- Lin P., Wei J., Yang Z.- L., Zhang Y. and Zhang K.: Snow data assimilation constrained land initialization improves seasonal temperature prediction, *Geophys. Res. Lett.*, 43, 11,423–11,432, doi: 10.1002/2016GL070966, 2016.

- Lin C., Chen D., Yang K., and Ou T.: Impact of model resolution on simulating the water vapor transport through the central Himalayas: implication for models' wet bias over the Tibetan Plateau. *Clim. Dyn.*, 51, 3195–3207, 2018.
- Liu S., Wu Q., Ren X., Yao Y., Schroeder S.R. and Hu H.: Modeled Northern Hemisphere Autumn and Winter Climate Responses to Realistic Tibetan Plateau and Mongolia Snow Anomalies, *J. Climate*, **30**, 9435–9454, 2017.
- 5 Lu M. et al.: Possible effect of the Tibetan Plateau on the “upstream” climate over West Asia, North Africa, South Europe and the North Atlantic, *Clim. Dyn.*, DOI 10.1007/s00382-017-3966-5, 2017.
- Maussion F., Scherer D., Mölg T., Collier E., Curio J. and Finkelnburg R.: Precipitation Seasonality and Variability over the Tibetan Plateau as Resolved by the High Asia Reanalysis., *J. Climate*, **27**, 1910–1927, <https://doi.org/10.1175/JCLI-D-13-00282.1>, 2014.
- 10 Ménégoz M., Gallée H. and Jacobi H. W.: Precipitation and snow cover in the Himalaya: from reanalysis to regional climate simulations, *Hydrol. Earth Syst. Sci.*, 17, 3921–3936, 2013.
- Onogi K. et al.: The JRA-25 re-analyses, *J. Met. Soc. Japan*, 85, 3, 369-432, 2007.
- Orsolini Y.J., Senan R., Balsamo G., Doblas-Reyes F., Vitart D., Weisheimer A., Carrasco A. and Benestad R.: Impact of snow initialization on sub-seasonal forecasts , *Clim. Dyn.*, DOI: 10.1007/s00382-013-1782-0, 2013.
- 15 Palazzi E., von Hardenberg J. and Provenzale A.: Precipitation in the Hindu-Kush Karakoram Himalaya: Observations and future scenarios, *J. Geophys. Res. Atmos.*, 118, 85–100, doi: [10.1029/2012JD018697](https://doi.org/10.1029/2012JD018697), 2013.
- Pomeroy J.W. and Li L.: Prairie and Arctic areal snow cover mass balance using a blowing snow model, *J. Geophys. Res.*, 105(D21): 26619–26634, 2000.
- Rai A., Saha S. K., Pokhrel S., Sujith K. and Halder S.: Influence of preonset land atmospheric conditions on the Indian summer monsoon rainfall variability, *J. Geophys. Res. Atmos.*, 120, 4551–4563, 2015.
- 20 Reichle R.H. et al.: Land Surface Precipitation in MERRA-2, *J. Climate*, 30, 1643-1664, 2017a.
- Reichle R.H., Draper C. S., Liu Q., Giroto M., Mahanama S. P. P., Koster R. D. and De Lannoy, G. J. M.: Assessment of MERRA-2 Land Surface Hydrology Estimates, *J. Climate*, 30, 2937–2960, 2017b.
- Riggs G.A. and Hall D. K.: MODIS Snow products Collection 6 User guide, 66pp, available from
- 25 https://icdc.cen.uni-hamburg.de/fileadmin/user_upload/icdc_Dokumente/MODIS/MODIS_Collection6_SnowCover_UserGuide_Dec2015.pdf, 2015.
- Sellers P.J., Mintz Y., Sud Y. C. and Dalcher A.: A Simple Biosphere Model (SIB) for Use within General Circulation Models. *J. Atmos. Sci.*, 43(6), 505–531, 1986.
- Senan R., Orsolini Y.J., Weisheimer A., Vitart F., Balsamo G., Stockdale T., Dutra E., Doblas-Reyes F. and Basang D.:
- 30 Impact of springtime Himalayan-Tibetan Plateau snowpack on the onset of the Indian summer monsoon in coupled seasonal forecasts, *Clim. Dyn.*, Vol. 47, 9, pp 2709–2725, doi:10.1007/s00382-016-2993-y, 2016.
- Stieglitz M., Ducharme A., Koster R. and Suarez M.: The Impact of Detailed Snow Physics on the Simulation of Snow Cover and Subsurface Thermodynamics at Continental Scales, *J. Hydrom.*, 2(3), 228–242, 2001.
- Su F. et al.: Evaluation of the Global Climate Models in the CMIP5 over the Tibetan Plateau, *J. Clim.*, 26, 3187-3208, 2013.

- Tiwari S., Kar S. C., Bhatla R.: Atmospheric moisture budget during winter seasons in the western Himalayan region, *Clim. Dyn.*, 48:1277–1295, 2017.
- Treichler D. et al.: High Mountain Asia glacier elevation trends 2003–2008, lake volume changes 1990–2015, and their relation to precipitation changes, *The Cryosphere Discuss.*, <https://doi.org/10.5194/tc-2018-238>, 2018.
- 5 Viste E. and Sorteberg A.: Snowfall in the Himalayas: An uncertain future from a little-known past, *The Cryosphere*, 9(3), 1147–1167, 2015.
- Wang A. and Zeng X.: Evaluation of multireanalysis products with in situ observations over the Tibetan Plateau, *J. Geophys. Res.*, 117, D05102, doi:[10.1029/2011JD016553](https://doi.org/10.1029/2011JD016553), 2012.
- Wang X., Wu C., Wang H., Gonsamo A., and Liu Z.: No evidence of widespread decline of snow cover on the Tibetan
10 Plateau over 2000–2015, *Scientific Reports*, vol. 7, Article number: 14645, 2017.
- Wang A., Wua R. and Huang G.: Low-frequency snow changes over the Tibetan Plateau, *Int. J. Climatol.*, 38: 949–963, 2018.
- Wegmann M., Orsolini Y., Dutra E., Bulygina O., Sterin A., and Brönnimann S.: Eurasian snow depth in long-term climate reanalysis, *The Cryosphere*, 11, 923–935, doi:10.5194/tc-11-923-2017, 2017.
- 15 Wright J. et al.: Chapter 2: SPARC Reanalysis Intercomparison Project (S-RIP) Description of the Reanalysis Systems, 2018.
- Wu G.X., Liu Y.M., He B., Bao Q., Duan A.M., Jin F.F.: Thermal Controls on the Asian Summer Monsoon, *Scientific Reports*, 2, doi: 10.1038/srep00404, 2012.
- 20 Wu G.X., Duan A.M., Liu Y.M., Mao J.Y., Ren R.C., Bao Q., He B., Liu B.Q. and Hu W.T.: Tibetan Plateau climate dynamics: recent research progress and outlook. *National Science Review*, 2, 100-116. doi: 10.1093/nsr/nwu045, 2015.
- Xiao Z.X. and Duan A.M.: Impacts of Tibetan Plateau Snow Cover on the Interannual Variability of the East Asian Summer Monsoon, *J. Climate*, 29, 8495–8514, <https://doi.org/10.1175/JCLI-D-16-0029.1>, 2016.
- Xue Y. et al.: Spring land surface and subsurface temperature anomalies and subsequent downstream late spring-summer
25 droughts/floods in North America and East Asia, *J. Geophys. Res.: Atmospheres*, 123, 5001–5019. <https://doi.org/10.1029/2017JD028246>, 2018.
- Yang K. et al.: Recent climate changes over the Tibetan Plateau and their impacts on energy and water cycle: A review, *Global and Planetary Change*, 112, 79–91, 2014.
- Yang J., Jiang L., Ménard C. B., Luoju K., Lemmetyinen J. and J. Pulliainen: Evaluation of snow products over the Tibetan
30 Plateau, *Hydrol. Process.* 29, 3247–3260, 2015.
- Yao T. et al.: Different glacier status with atmospheric circulations in Tibetan Plateau and surroundings, *Nature Climate Change*, 2, 663–667, 2012.
- Zhang Y., Li T. and Wang B.: Decadal change of the spring snow depth over the Tibetan Plateau: The associated circulation and influence on the East Asian summer monsoon, *J. Climate*, 17, 2780-2793, 2004.

Zhang G. et al.: Extensive and drastically different alpine lake changes on Asia's high plateaus during the past four decades, *Geophys. Res. Lett.*, 44, 252–260, doi:10.1002/2016GL072033, 2017.

Zhou X., Yang K., Beljaars A., Li H., Lin C., Huang B., Wang Y.: Dynamical impact of parameterized turbulent orographic form drag on the simulation of winter precipitation over the western Tibetan Plateau, *Clim. Dyn.*,
5 <https://doi.org/10.1007/s00382-019-04628-0>, 2019.

Zou H. et al.: Validation and application of reanalysis temperature data over the Tibetan Plateau, *J. Meteor. Res.*, 28(1), 139-149, 2014.

Appendix

10 1. ERA-Interim

Snow is represented as a single bulk layer on top of the soil column with prognostic temperature, mass, density and albedo. Snow density is constant with depth, increasing exponentially with snow age, and decreasing after snowfall events assuming a constant snowfall density of 100 kg m^{-3} . Snow albedo reduces exponentially as snow ages over low vegetation or bare soil, but is constant in time for snow under high vegetation, and is reset to a maximum value of 0.85 after snowfall event.

15 A snow depth analysis is performed using a Cressman (1959) interpolation with successive corrections. Station observations of snow depth are used, however there are no stations used over the TP. Gridded snow cover from IMS is also assimilated since 2004, using the coarser 24-km resolution product as detailed in Drusch et al. (2004). The snow depth analysis is relaxed toward a climatology when observations are unavailable.

Snow cover fraction is a diagnostic variable derived from the relation

20 $\text{SCF} = \min(1, \text{SWE}/15)$ where SWE is the snow mass (kg m^{-2}). A layer of 15 kg m^{-2} represents 100 % snow cover (15 cm depth considering a snow density of 100 kg m^{-3} , or 5 cm depth if considering a snow density of 300 kg m^{-3}).

2. ERA5

The snow model is also a bulk single layer as in ERA-I, with the same prognostic variables but with several modifications, in particular a diagnostics of snow liquid water content, a revised SCF formulation and snow density evolution (Dutra et al.,
25 2010). A two-dimensional optimal interpolation snow analysis, including the water equivalent, temperature and density of snow is performed using station observations of snow depth and the gridded SCF product from IMS 4-km resolution product (de Rosnay et al., 2014; 2015). Unlike ERA-I, IMS data is not used above 1500 m, i.e. in high altitude regions, which includes the TP. No station data over the TP is used. Unlike ERA-I, the snow depth analysis is not relaxed toward a climatology when observations are unavailable.

30 Snow cover fraction is a diagnostic variable derived from the relation

$\text{SCF} = \min(1, \text{SD}/10)$ where SD is the snow depth in cm so that a layer of 10 cm represents 100 % snow cover.

3. ERA5L-CTRL and dedicated experiments

We made several additional off-line simulations of the HTESSSEL model forced by meteorological data from ERA5. The land model is hence the same as used in ERA5 but there is no assimilation of snow or land observations, contrarily to the ERA5 re-analyses. A simple parametrization of snow sublimation due to blowing snow, as proposed by Gordon et al. (2006) and used in Brun et al. (2013), is newly implemented in HTESSSEL. The sublimation of blowing snow (Q_s , $\text{kg m}^{-2} \text{s}^{-1}$) is
5 computed as in Gordon et al. (2006):

$$Q_s = A \left(\frac{T_0}{T_a} \right)^\gamma U_t \rho_a q_{sa} (1 - Rh_a) \left(\frac{U_a}{U_t} \right)^B, U_a > U_t$$

where A and B are dimensionless constants ($A=0.0018$, $B=3.6$), $\gamma=4$, T_0 is the water freezing temperature. The formulation requires the lowest model level (at 10 m height) fields of air temperature (T_a), air density (ρ_a), wind speed (U_a), relative humidity (Rh_a) and saturation specific humidity (q_{sa}). U_t (m s^{-1}) is the threshold for initiation of blowing snow also used by
10 Gordon et al (2006) following Li and Pomeroy (1997)

$$U_t = 6.98 + 0.0033(T_a - 245.88)^2$$

In the experiments with reduced wind threshold, the first coefficient (6.98) is replaced by 5. This simple parametrization only represents the snow mass removal by sublimation due to the blowing of snow, but it does not account for the change in the energy budget. Hence, the energy required to sublimate the snow is not taken from the surface or from the lower
15 atmosphere. While this approximation would not be valid in a coupled land-atmosphere simulation, it seems appropriate in an off-line simulation. Other experiments tested the impacts of the threshold in snow cover conversion (see SD parameter in the description of ERA5 above) and of reducing snowfall by half. The experiments are summarized in Table 4.

4. JRA-55

The land surface model in JRA-55 is the Simple Biosphere model (SiB) (Sellers et al. 1986) which represents snow mass on
20 the ground and its evolution by updating several parameters and calculations. A separate optimal interpolation-based snow depth analysis is performed once per day (at 18UTC). The first-guess background state combines the land-surface analysis and Special Sensor Microwave/ Imager (SSM/I) and the Special Sensor Microwave Imager Sounder (SSMIS) snow cover satellite observations. The analysis also considers in-situ observations of snow depth over China from CMA archives, including a dozen stations over the TP (Onogi et al., 2007; Kobayashi et al., 2015).

25 Snow cover fraction is a diagnostic variable derived from the relation

$$\text{SCF} = (\min(1, (\text{SD})/2)) \text{ where SD is the snow depth in cm, so that a layer of 2 cm represents 100 \% snow cover.}$$

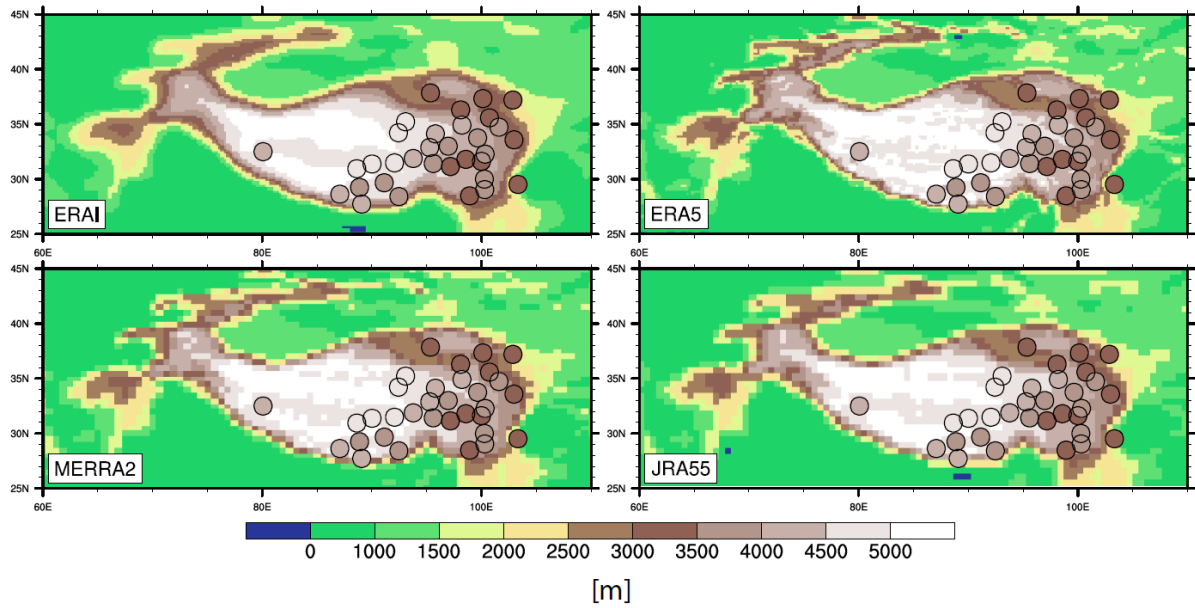
5. MERRA-2

The evolution of snow mass, depth and heat content is simulated within each catchment using a three-layer snow model
30 (Reichle, et al., 2017b). Density in each layer evolves via parameterized representations of compaction due to snow overburden and melting/refreezing (Stieglitz et al. 2001). Snow is redistributed among layers as necessary to keep the surface layer shallow enough to respond to diurnal variability. The albedo of snow-covered land surface depends on snow density and vegetation type.

No snow data assimilation is performed. However, MERRA-2 performs an on-line correction for precipitation using two different, gridded precipitation datasets from NOAA Climate Prediction Center, namely the Unified Gauge-Based Analysis of Global Daily Precipitation (CPCU) product and the Merged Analysis of Precipitation (CMAP) product (Reichle et al., 2017a,b).

- 5 Snow cover fraction is a diagnostic variable derived from the relation

$SCF = \min(1, SWE/26)$, where SWE is the snow mass in kg m^{-2} . A layer of 26 kg m^{-2} represents 100 % snow cover (i.e., a 26-cm snow depth considering a density of 100 kg m^{-3}).



5 **Figure 1: Topographic maps of the TP region (altitude in m) at the horizontal resolution of each re-analysis. The locations of the 33 stations are also shown with the coloured circles indicating the altitude range.**

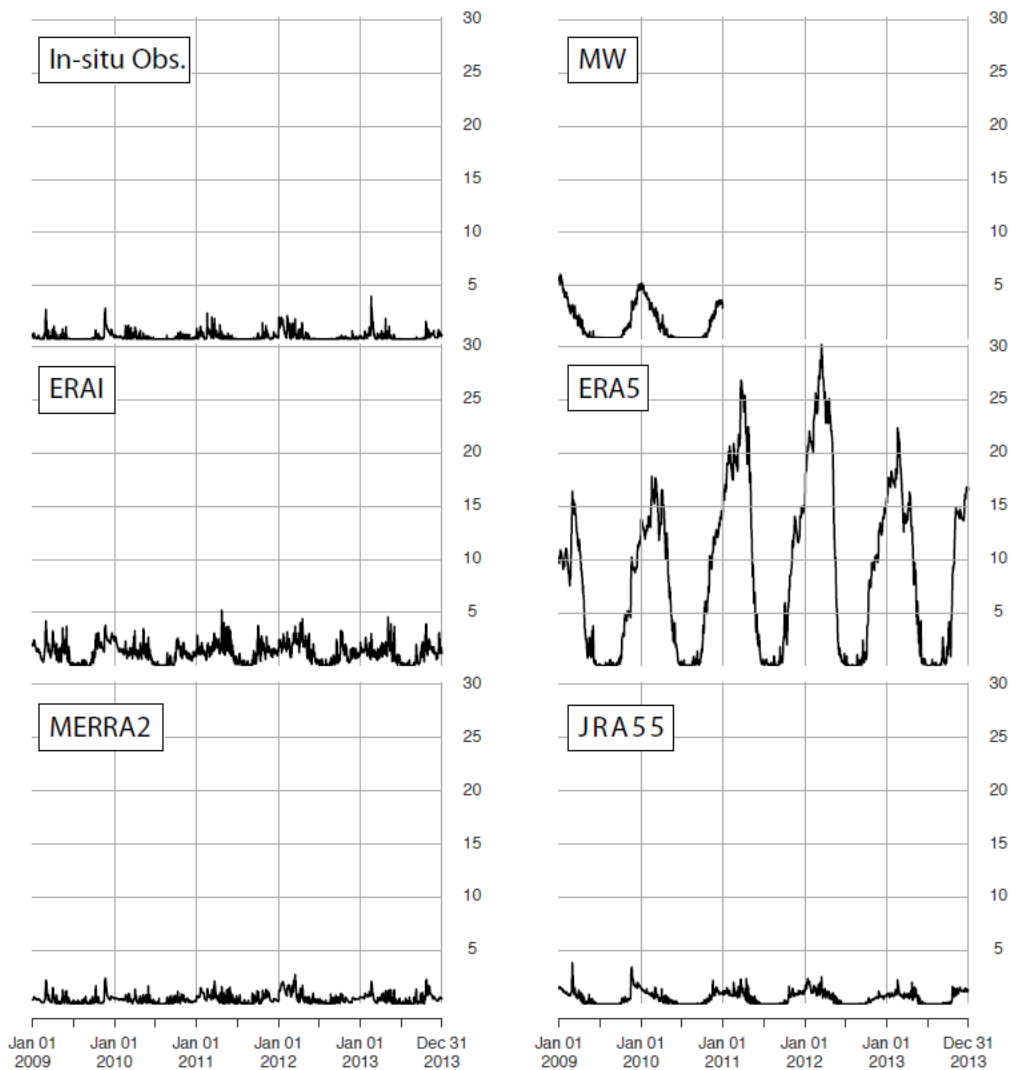


Figure 2: Comparison over the 5-year period 2009-2013 of daily SD [in cm] between the observations, comprising both in-situ station and MW data (over 2009 and 2010), and the 4 re-analyses collocated at the station coordinates, namely ERA5, ERA-I, MERRA-2 and JRA-55. The average is carried out over the 33 stations shown in Fig. 1.

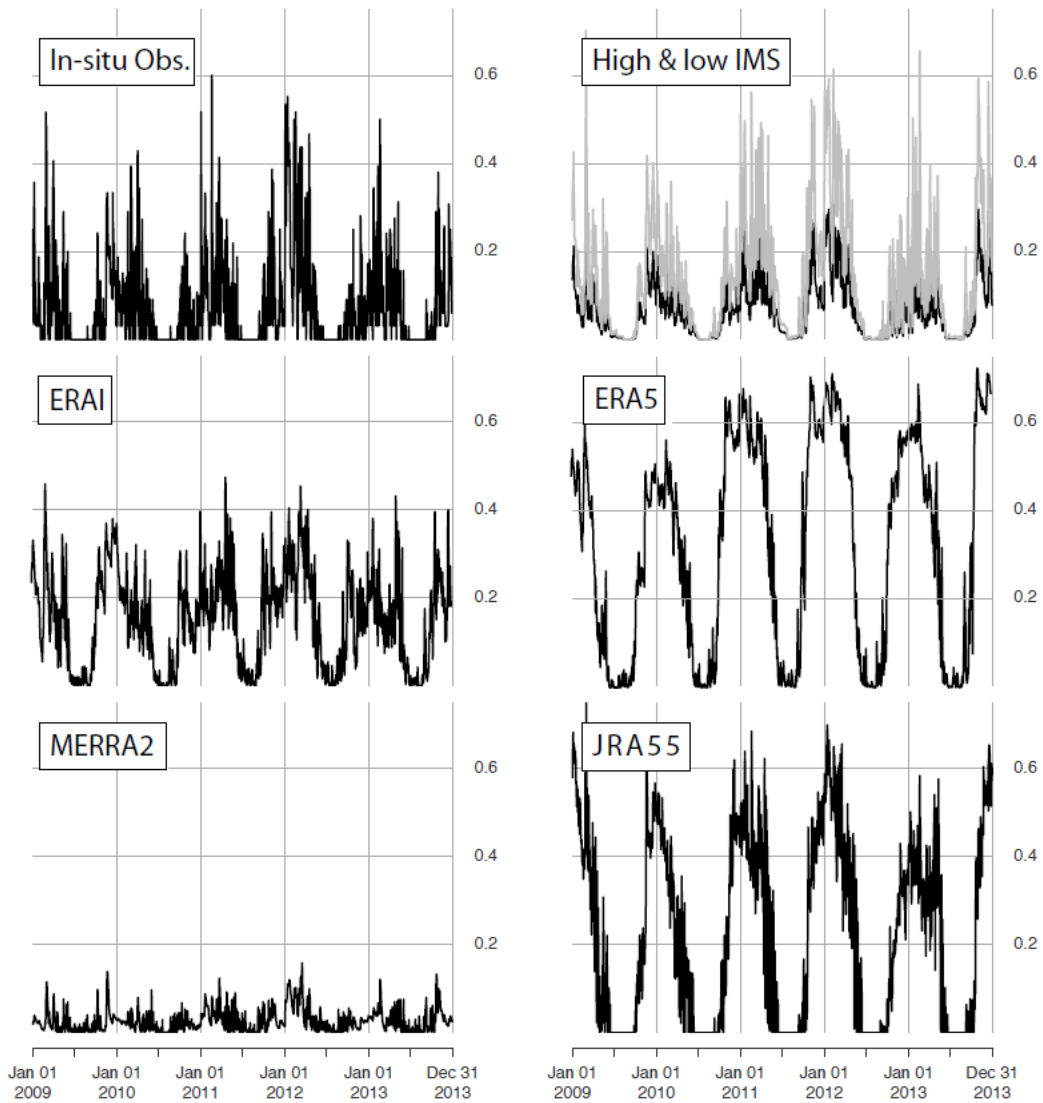
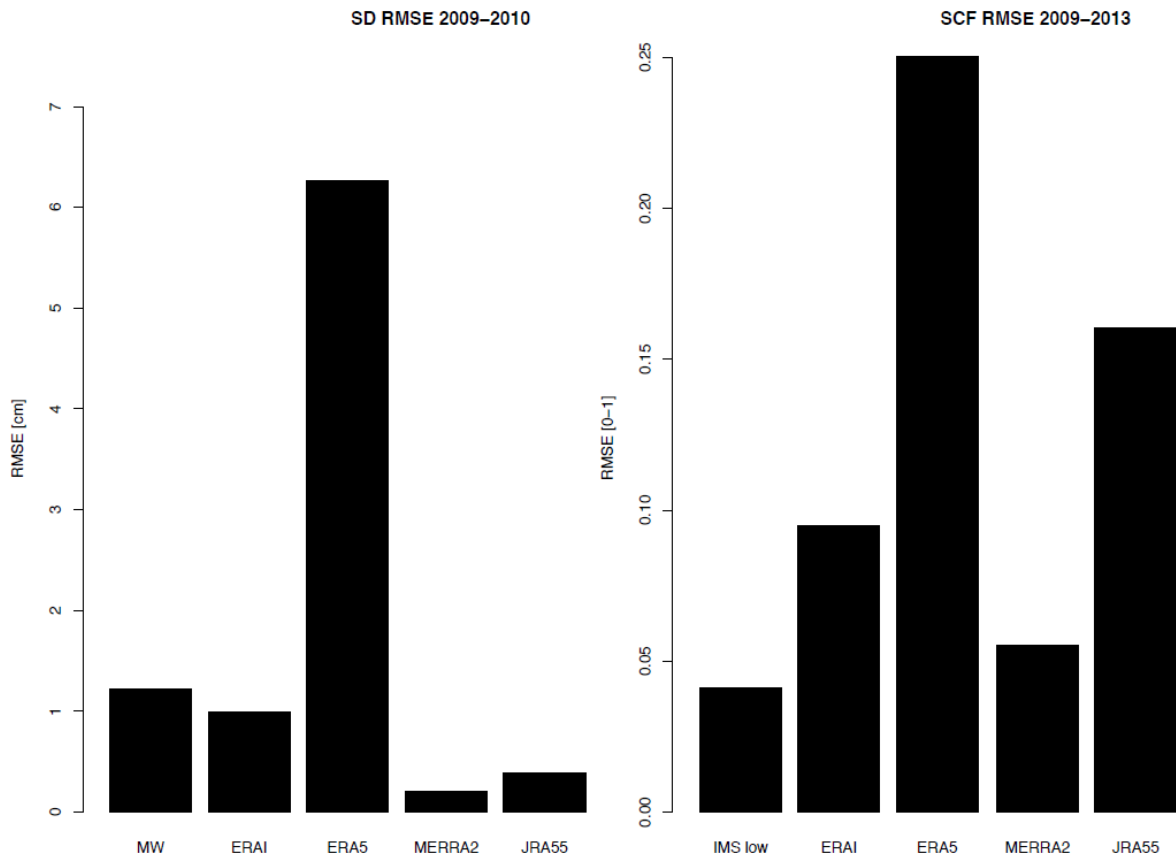


Figure 3: Comparison of daily SCF [between 0 and 1] over the 5-year period 2009-2013 between the observations, comprising both the in-situ station and IMS satellite data, with the 4 re-analyses analyses collocated at the station coordinates, namely ERA5, ERA-I, MERRA-2 and JRA-55. The data has been averaged over the 33 stations. The IMS data is represented by the low and high estimates, resulting from converting the binary 4-km data to a grid comparable to the re-analyses resolution.

5



5 **Figure 4: Estimate of the root-mean-square error (RMSE) between daily station data and collocated re-analyses or satellite observations for SD [in cm] (left panel) over the two years when satellite MW data is available (2009 and 2010), and for SCF [between 0 and 1] (right panel), over the 5-year period (2009-2013).**

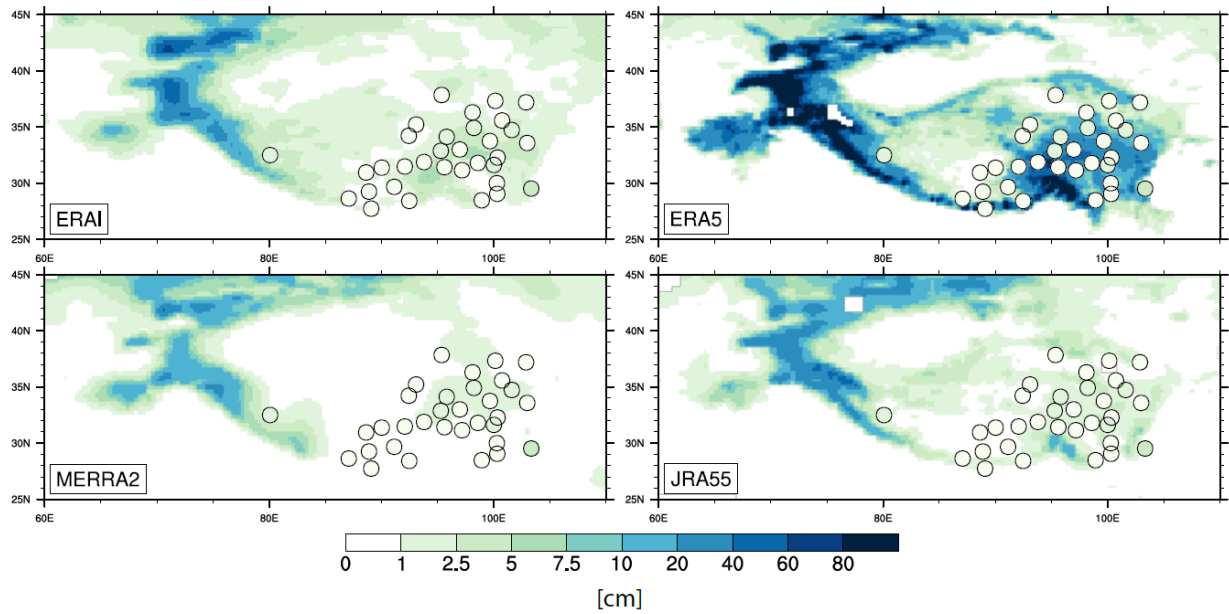


Figure 5: Maps of the 5-year mean SD [in cm] over the TP region in January for each of the 4 re-analyses (ERA5, ERA-I, MERRA-2 and JRA-55) with the in-situ SD [in cm] embedded locally in each map.

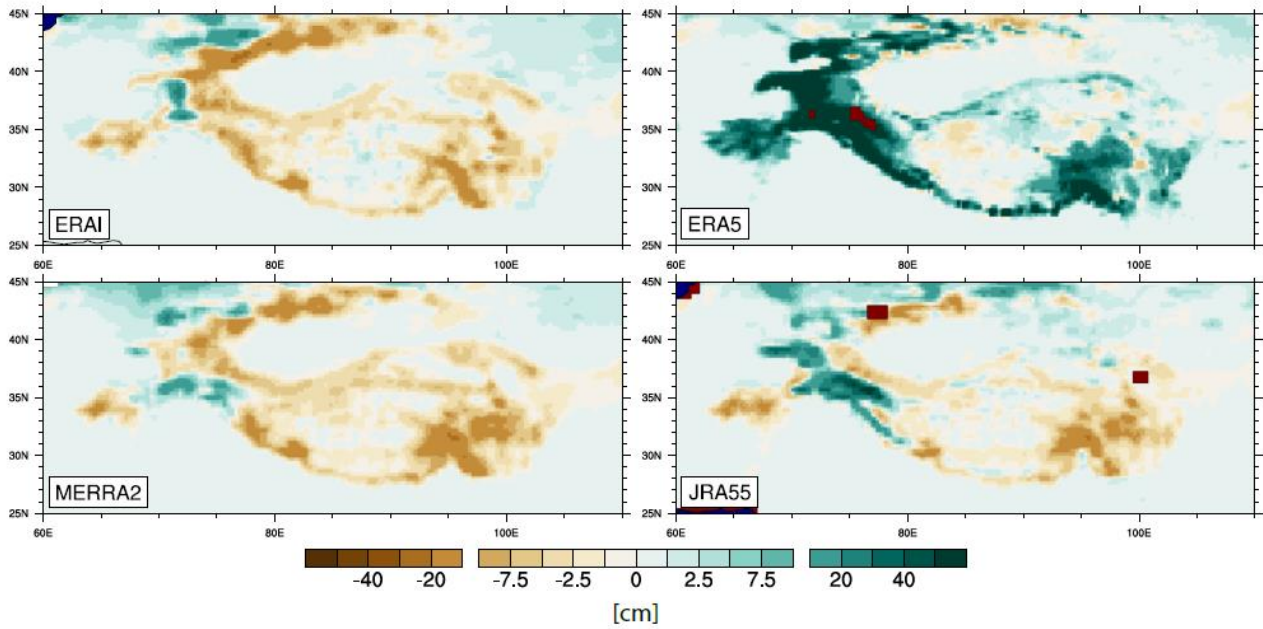


Figure 6: Maps of the 2-year mean SD January anomalies [in cm] from the satellite MW data for the years 2009 and 2010 over the TP region for each of the 4 re-analyses (ERA5, ERA-I, MERRA-2 and JRA-55).

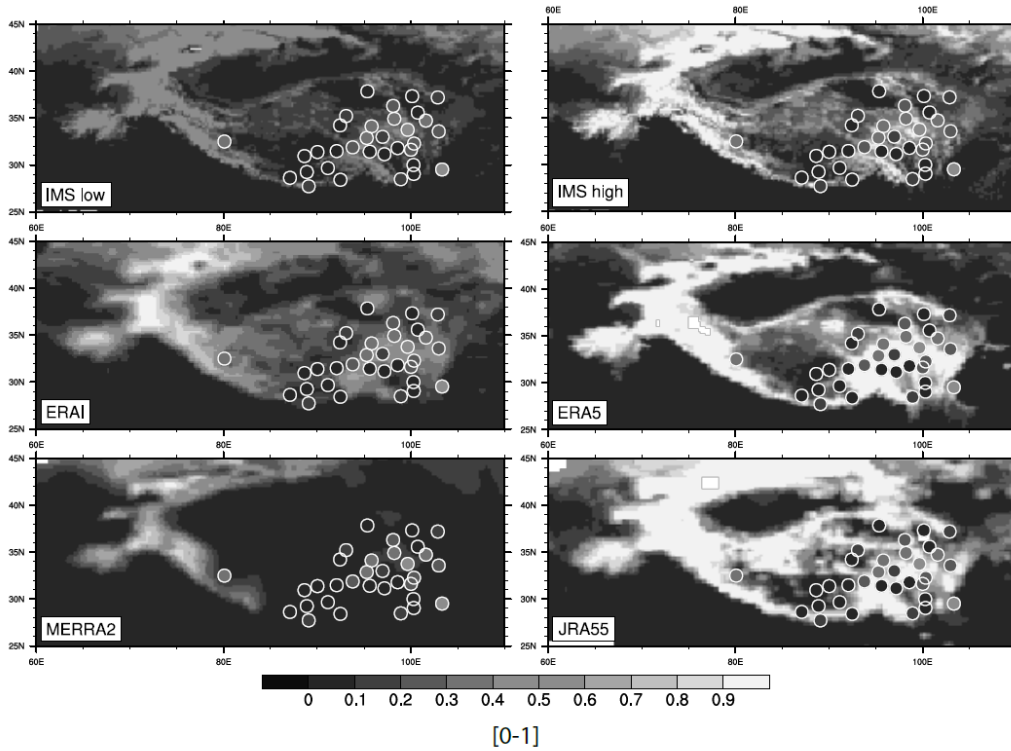


Figure 7: Maps of the 5-year mean SCF [between 0 and 1] over the TP region in January for the IMS satellite data (two maps for the high and low estimates) and for each of the 4 re-analyses (ERA5, ERA-I, MERRA-2 and JRA-55), with the in-situ SCF observations [between 0 and 1] embedded locally in each map.

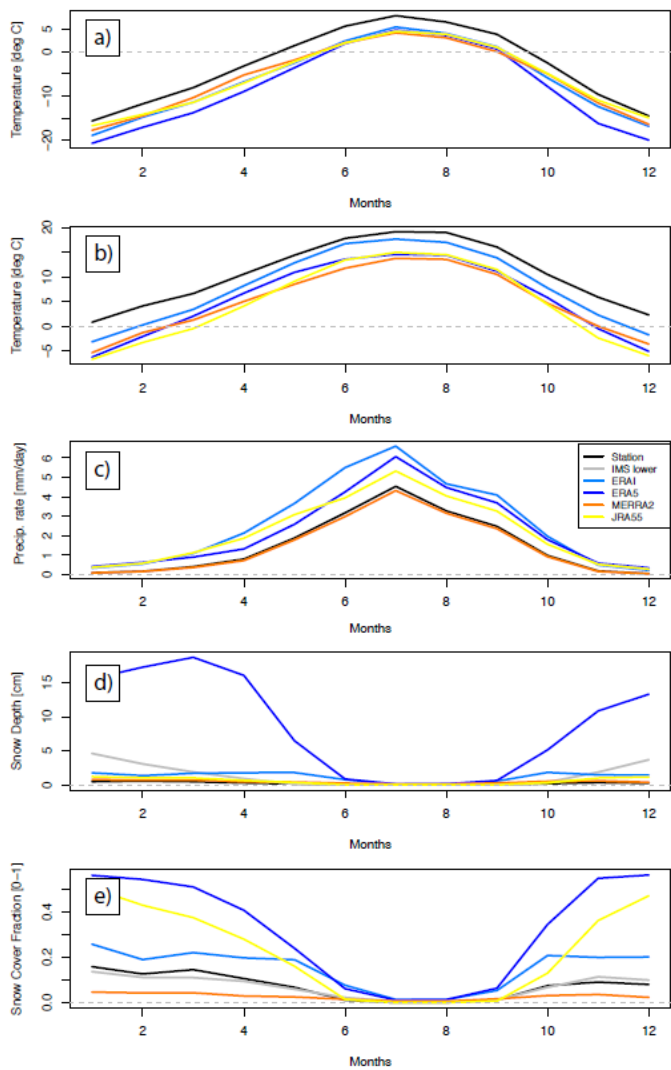


Figure 8: The 5-year mean (2009-2013) monthly-mean seasonal cycle for minimum temperature [in deg C] (a), maximum temperature [in °C] (b), precipitation rate [in mm per day] (c), SD [in cm] (d) and SCF [between 0 and 1] (e), averaged over all the 33 stations. The label Satellite refers to IMS (low estimate) for snow cover, or to MW for snow depth.

5

10

Table 1: General characteristics of the re-analyses

	ERA-Int	ERA5	Offline-ERA5L-CTRL	MERRA-2	JRA-55
Approximate Spatial resolution	~79km	~32km	~9km	~50km	~55km
Land Model version	TESSEL	HTESSEL	HTESSEL-CY43R1	Catchment LSM	SIB
Atmospheric Model	IFS Cy31r2	IFS Cy41r2	NONE	GEOS 5.12.4	JMA GSM
Assimilated snow data	In-situ (but not on TP), IMS (24 km)	In-situ (but not on TP), IMS (4 km)	NONE	NONE	In-situ (also on TP), MW (SSM-I, SSMIS) snow cover
Snow model	1-layer	1-layer	1-layer	3-layer	1-layer

5

Snow depth	IN-SITU	MW	MERRA2	JRA55	ERA-I	ERA5
IN-SITU	1					
MW	0.32	1				
MERRA2	0.75	0.32	1			
JRA55	0.72	0.81	0.67	1		
ERA-I	0.53	0.48	0.68	0.6	1	
ERA5	0.51	0.76	0.58	0.75	0.57	1

Snow cover	IN-SITU	IMS	MERRA2	JRA55	ERA-I	ERA5
In-SITU	1					
IMS	0.78	1				
MERRA2	0.63	0.78	1			
JRA55	0.73	0.76	0.57	1		
ERA-I	0.59	0.74	0.7	0.67	1	
ERA5	0.58	0.8	0.89	0.6	0.77	1

5 Table 2: Temporal correlation matrix between in-situ observations and re-analyses or satellite data, for daily SD (top) and daily SCF (bottom). The IMS low-estimate has been used. Correlations are calculated over the whole 5-year period, except for MW SD data when the two years 2009 and 2010 are used, and averaged over the 33 stations.

10

15

Snow cover days	5-year mean	2009	2010	2011	2012	2013
In-SITU	3.08	3.06	2.31	3.28	3.81	2.92
IMS	3.20	2.58	1.90	4.26	3.80	3.47
MERRA2	0.03	0.06	0.02	0.015	0.05	0.02
JRA55	7.31	7.28	6.24	8.21	7.30	7.50
ERA-I	2.95	3.16	2.20	3.38	3.31	2.73
ERA5	8.99	4.92	8.77	10.70	10.44	10.14

	IN- SITU	IMS	MERRA2	JRA55	ERA-I	ERA5
IN-SITU	1					
IMS	0.88	1				
MERRA2	0.29	0.15	1			
JRA55	0.81	0.86	0.18	1		
ERA-I	0.84	0.79	0.34	0.72	1	
ERA5	0.78	0.82	0.11	0.86	0.73	1

Table 3: Values of the annual means of monthly snow cover days averaged during the whole 5-year period (the 2nd column) and during 2009 to 2013 (the 3rd to 7th columns), respectively (top), for each dataset. Temporal correlation matrix between in-situ observations and re-analyses for monthly SCD during the whole 5-year period (bottom). The SCDs are defined as the days when the SCF is greater than 0.5, and are averaged over the 33 stations.

10

15

Experiment	Description
ERA5L-CTRL	Land-only simulation with the same configuration as ERA5 in the land-surface
BLW	Including the effect of sublimation due to blowing snow as in Gordon et al. 2006
BLW_L	As BLW, but changing the critical threshold for initiation from 6.98 to 5 m s ⁻¹
SCF05	Using 5 cm instead of 10 cm threshold for 100% snow cover fraction
SCF20	Using 20 cm instead of 10 cm threshold for 100% snow cover fraction
SNF50	Reducing the snowfall rate by 50%

Table 4. Details of the off-line ERA5-land experiments.

Experiment	Snow depth (cm)	Snow cover (0-1)	Sublimation (mm)	Sublimation blowing (mm)	Snow melt (mm)	Snowfall (mm)	Rainfall interception (mm)
ERA5	9.16	0.33	-	-	-	204.06	-
ERA5L-CTRL	8.54	0.29	-37.34	0.00	-184.13	204.06	17.42
BLW	8.50	0.29	-36.29	1.17	-183.82	204.06	17.40
BLW_L	8.39	0.28	-35.17	-3.44	-182.74	204.06	17.30
SCF05	7.46	0.29	-37.74	0.00	-182.76	204.06	16.45
SCF20	11.71	0.32	39.17	0.00	-184.16	204.06	19.27
SNF50	1.38	0.12	-24.03	0.00	84.15	102.03	6.16
OBS	0.23	0.13					

Table 5: ERA5 and off-line ERA5-land experiments mean annual snow and associated fluxes averaged over the 33 stations.

The fluxes are the annual mean accumulated: snow sublimation, snow sublimation due to blowing snow, snow melt, snowfall and rainfall intercepted in the snowpack. The last row (OBS) presents the mean snow depth derived from the station data, and the mean snow cover from the IMS satellite data (low estimate).

Experiments	Snow depth RMSE (cm)	Snow cover RMSE (0-1)	Snow depth correlation	Snow cover correlation
ERA5	11.98	0.25	0.51	0.78
ERA5L-CTRL	11.19	0.21	0.50	0.80
BLW	11.13	0.20	0.50	0.80
BLW_L	10.97	0.20	0.50	0.80
SCF05	9.94	0.20	0.50	0.81
SCF20	14.98	0.25	0.51	0.77
SNF50	1.58	0.08	0.60	0.79

5

Table 6. Root mean square error (RMSE) and temporal correlation for snow depth (versus stations data) and snow cover (versus IMS satellite) for ERA5 and the different experiments. The time series of the observation and experiments were first averaged over the 33 stations before the score calculations.

10

15